Regulation of Exocytosis by Protein Kinases and Ca^{2+} in Pancreatic Duct Epithelial Cells

Duk-Su Koh,* Mark W. Moody,‡ Toan D. Nguyen,‡ and Bertil Hille*

From the *Department of Physiology and Biophysics, and ‡Department of Medicine, School of Medicine, University of Washington, Seattle, Washington 98195-7290

ABSTRACT We asked if the mechanisms of exocytosis and its regulation in epithelial cells share features with those in excitable cells. Cultured dog pancreatic duct epithelial cells were loaded with an oxidizable neurotransmitter, dopamine or serotonin, and the subsequent release of these exogenous molecules during exocytosis was detected by carbon-fiber amperometry. Loaded cells displayed spontaneous exocytosis that may represent constitutive membrane transport. The quantal amperometric events induced by fusion of single vesicles had a rapid onset and decay, resembling those in adrenal chromaffin cells and serotonin-secreting leech neurons. Quantal events were frequently preceded by a "foot," assumed to be leak of transmitters through a transient fusion pore, suggesting that those cell types share a common fusion mechanism. As in neurons and endocrine cells, exocytosis in the epithelial cells could be evoked by elevating cytoplasmic Ca^{2+} using ionomycin. Unlike in neurons, hyperosmotic solutions decreased exocytosis in the epithelial cells, and giant amperometric events composed of many concurrent quantal events were observed occasionally. Agents known to increase intracellular cAMP in the cells, such as forskolin, epinephrine, vasoactive intestinal peptide, or 8-Br-cAMP, increased the rate of exocytosis. The forskolin effect was inhibited by the Rp-isomer of cAMPS, a specific antagonist of protein kinase A, whereas the Sp-isomer, a specific agonist of PKA, evoked exocytosis. Thus, PKA is a downstream effector of cAMP. Finally, activation of protein kinase C by phorbol-12-myristate-13-acetate also increased exocytosis. The PMA effect was not mimicked by the inactive analogue, 4α-phorbol-12,13-didecanoate, and it was blocked by the PKC antagonist, bisindolylmaleimide I. Elevation of intracellular Ca^{2+} was not needed for the actions of forskolin or PMA. In summary, exocytosis in epithelial cells can be stimulated directly by Ca^{2+}, PKA, or PKC, and is mediated by physical mechanisms similar to those in neurons and endocrine cells.

KEY WORDS: secretion • secretagogue • cyclic AMP • photometry • amperometry

INTRODUCTION

In neurons and some endocrine cells, Ca^{2+} plays a pivotal role as the final signal for rapid stimulus-evoked release of neurotransmitters and hormones. An elevation of intracellular Ca^{2+} will also trigger exocytosis in various nonexcitable cells (Morimoto et al., 1995; Coorssen et al., 1996). Nevertheless, although the machinery of exocytosis uses related universal molecular components, Ca^{2+} may not be the physiological signal for exocytosis in all nonneuronal cells. For example, in neutrophils, eosinophils, and mast cells, the intracellular signal for exocytosis and degranulation seems not to be Ca^{2+}, protein kinase A, or protein kinase C (Neher and Almers, 1986; Almers and Neher, 1987; Scepek et al., 1998). On the other hand, the hormonal regulation of secretion in various gastrointestinal and airway epithelial cells is described as using cAMP or PKC, depending on the stimulating hormone (Forstner et al., 1993; Larivee et al., 1994; Klinkspoor et al., 1996; Oda et al., 1996; Abdullah et al., 1997; Urushidani and Forte, 1997; Brown et al., 1998; Fujita-Yoshigaki, 1998; reviewed in Hille et al., 1999). To compare this kind of exocytosis with that in neurons, we decided to investigate properties of exocytosis in cultured dog pancreatic duct epithelial cells using amperometry. In these cells, roles for cAMP and Ca^{2+} in mucin secretion are known (Oda et al., 1996; Nguyen et al., 1998). The principal questions were whether PKA, PKC, and Ca^{2+} all can trigger secretion in one cell type and whether they act independently.

METHODS

Chemicals

Stock solutions of 20 mM forskolin, 20 mM H-89, 100 μM phorbol-12-myristate-13-acetate, and 500 μM bisindolylmaleimide I (BIS)[1] were prepared in dimethyl sulfoxide. Stock solutions of 1 mM epinephrine, 1 mM vasoactive intestinal peptide (VIP), and 1 M cAMP analogues were made up in saline solution. The cAMP

Portions of this work were previously published in abstract form (Koh, D.-S., M.W. Moody, T.D. Nguyen, B.L.Tempel, and B. Hille. 1997. *Soc. Neurosci. Abstr.* 22:467).

Address correspondence to Bertil Hille, Department of Physiology and Biophysics, G-424 Health Sciences Building, University of Washington, Seattle, Box 357290, WA 98195-7290. Fax: 206-685-0619; E-mail: hille@u.washington.edu

[1]*Abbreviations used in this paper:* BAPTA, 1,2-bis-(2-aminophenoxy)ethane-*N,N,N′,N′*-tetraacetic acid; BIS, bisindolylmaleimide I; VIP, vasoactive intestinal peptide.

analogues included 8-Br-cAMP and the Rp and Sp optical enantiomers of 8-Br-cAMPS. Rp-8-Br-cAMPS, Sp-8-Br-cAMPS, H-89, PMA, and BIS were purchased from Calbiochem. VIP was from Bachem. Serotonin-HCl and dopamine-HCl were from RBI. Other chemicals were from Sigma-Aldrich.

Cell Culture

The derivation and culture of pancreatic epithelial cells from the main pancreatic duct of the dog has been described (Oda et al., 1996). Although the cells are not a transformed cell line, they can be repeatedly subcultured. In brief, the cells were cultured in Vitrogen (Collagen)-coated Transwell inserts (3-μm pore size, 24-mm diameter; Corning Costar), and the inserts were placed above a confluent feeder layer of human gallbladder myofibroblasts. The cells were maintained in Eagle's minimum essential medium with 10% fetal bovine serum plus insulin-transferrin-sodium selenite medium supplement from Sigma Chemical Co. When confluent, the cells were treated with 2.5% trypsin/EDTA at 37°C for 30 min and passaged (10^5 cells per well) to new coated inserts with fresh feeder layers.

For single-cell experiments, cells were plated on small coverglass chips (5 × 5 mm) coated with a thick layer of Vitrogen. The cells were fed with medium conditioned by gallbladder myofibroblasts. Experiments were performed with cells between 2 and 7 d after plating. Although the epithelial cells we use can form well differentiated monolayers with apical-basolateral polarity, our experiments were carried out on subconfluent epithelial cells that were presumably not completely differentiated or polarized.

Loading of Monoamines and Amperometric Measurement of Exocytosis

We used carbon-fiber amperometry to detect exocytosis from single cells in real time (Kawagoe et al., 1993; Chow and von Rüden, 1995). Amperometry provides high resolution to detect molecules released from single secretory vesicles and stability for long recordings. Since the method measures only exocytosis, it can detect infrequent exocytotic events without being disturbed by concurrent endocytosis. Amperometric measurements are normally limited to cells that package and secrete an endogenous oxidizable molecule such as catecholamines or serotonin; however, in some cases oxidizable molecules can be introduced artificially. Thus, Smith et al. (1995) and Zhou and Misler (1996) demonstrated the feasibility of loading serotonin exogenously via the serotonin transporter into pancreatic β cells by incubating overnight with 0.5–1-mM concentrations of serotonin. We have found that soaking a variety of cells in 50–100× higher concentrations of amines such as dopamine or serotonin will force the exogenous molecules to distribute passively into cytoplasm and acidic secretory vesicles (Billiard et al., 1997; Koh et al., 1997; Kim et al., 2000). This loading process does not need amine transporters in the plasma and vesicular membranes and therefore can be used in principle for most cell types, but the exogenous molecules probably end up in a range of types of intracellular acidic compartments.

For loading, cells were incubated for 40 min at room temperature in a solution containing (mM): 70 serotonin or dopamine, 68 NaCl, 2.5 KCl, 2 $CaCl_2$, 1 $MgCl_2$, 10 D-glucose, and 10 HEPES, pH 7.3 with NaOH. The cells were then transferred to culture medium and kept at 37°C, 5% CO_2 for up to 4 h. Experiments were performed in a monoamine-free saline solution containing (mM): 138 NaCl, 2.5 KCl, 2 $CaCl_2$, 1 $MgCl_2$, 10 D-glucose, and 10 HEPES, pH 7.3 with NaOH.

Vesicular release of catecholamine was monitored as pulses of electric current generated by oxidation of the molecules at the tip of a carbon-fiber electrode polarized at +600 mV. Carbon-fiber microelectrodes were fabricated from 5–11-μm carbon fibers (PAN T650 or P25; Amoco Performance Products) and polypropylene 10 μl micropipettor tips as described by Koh and Hille (1999). Application of +600 mV to a fresh electrode in the bath elicited an initial transient polarization current. Measurements were begun after this electrode current fell below 10 pA. The amperometric currents were recorded with EPC 5 or EPC 9 (HEKA Elektronik) patch-clamp amplifiers, filtered at 10 kHz (−3 dB cut off frequency) using a four-pole Bessel filter (Ithaco Co.), digitized, and stored on video tape. For analysis, the recordings were replayed, filtered, digitized, and stored by a computer. The final filter frequency was 100 Hz except where indicated. The sampling rate was four or five times faster than the filter frequency. In simultaneous recordings of $[Ca^{2+}]_i$ and amperometry, illumination of the carbon-fiber probe with ultraviolet light produced small current artifacts that were digitally corrected when larger than the baseline noise level (see Figs. 2, 4, and 7).

Solutions were exchanged by a local perfusion system that allows complete exchange of medium bathing the cells within 2 s.

Single-Cell Photometry

The intracellular Ca^{2+} concentration ($[Ca^{2+}]_i$) was measured with the Ca^{2+}-sensitive fluorescent dye indo-1 loaded into cells such as the membrane-permeable AM ester (Molecular Probes, Inc.). The cells were incubated for 30 min in saline solution with 1 μM indo-1 AM at room temperature. The excitation wavelength was 365 nm (100 W mercury lamp), and fluorescence signals were recorded at 405 and 500 nm, using a pair of photon-counting photomultiplier tubes. The sample rate was 0.5 Hz for photometry alone and 0.1 Hz for simultaneous photometry and amperometry. Background fluorescence measured from a cell-free area was corrected. The $[Ca^{2+}]_i$ was calculated using the equation: $[Ca^{2+}]_i = K^* (R - R_{min})/(R_{max} - R)$, where R is the 405/500-nm fluorescence ratio and R_{min} and R_{max} are the ratios for Ca^{2+}-free and -bound dye, respectively (Grynkiewicz et al., 1985). R_{min}, R_{max}, and K^* were measured on cells perfused with Na^+-rich external solutions containing 20 μM ionomycin plus 50 mM EGTA or 20 mM Ca^{2+}, or 20 mM EGTA and 15 mM Ca^{2+} for >15 min. In addition, 5 μM thapsigargin and 2 μM carbonyl cyanide m-chlorophenylhydrazone were included in all calibration solutions to block active clearance of Ca^{2+} from the cytoplasm. The calculated free $[Ca^{2+}]$ in the 20 mM EGTA and 15 mM $CaCl_2$ solution was 251 nM. Values for R_{min}, R_{max}, and K^* were 0.44, 4.46, and 1,770 nM, respectively (n = 8–13 cells for each measurement).

For measuring $[Ca^{2+}]_i$ levels higher than several micromolar, some cells were loaded with the low-affinity dye, mag-indo-1. Loading of the dye was performed as for indo-1, except for a shorter loading time (5–10 min). The calibration solutions were the same, except the mid-point solution contained 10 mM nitrilotriacetic acid and 5 mM Ca^{2+} with a calculated free $[Ca^{2+}]$ of 100 μM. Values for R_{min}, R_{max}, and K* for mag-indo-1 dye were 0.19, 1.90, and 327 μM, respectively (n = 7–18 cells).

Data Analysis

Amperometric recordings were semiautomatically analyzed using software written in Igor (WaveMetrics). Some recordings with a small number of amperometric signals were plotted on a fast chart recorder and events were counted manually. The rate of exocytosis was defined as the number of amperometric spikes per 30-s time bin. To evaluate relative exocytosis, the rates of exocytosis in control and test conditions were averaged for 2 min. As the maximal exocytosis is reached at different times in different test solutions, the 2-min analysis period was taken after various time delays: 3 min for forskolin or PMA on 1,2-bis-(2-aminophenoxy)ethane-*N,N,N,N*-tetraacetic acid (BAPTA)–loaded cells (see

Figs. 4, and 6–8), Rp-8-Br-cAMPS (see Fig. 6) or BIS (see Fig. 8) treatments, 2 min for forskolin, PMA or Sp-8-Br-cAMPS on cells not loaded with BAPTA (see Figs. 5, 6, and 8), and 1 min for 2 mM Ca^{2+} on ionomycin- (see Fig. 2) and hyperosmotic solution-treated (see Fig. 10) cells. During treatments with hyperosmotic solution, only the last minute of the recordings was analyzed. Relative exocytosis was defined by the ratio of exocytosis rates after and before treatments.

Kinetics of single quantal events were fitted with the sum of two exponential functions using events without a foot. Rise times (10–90% of peak amplitude) and fall times (90–10% of peak amplitude) were extracted from the fitted curves. Half-width was measured as time spent above 50% of peak amplitude.

All numerical values are given as mean ± SEM. The significance of differences between mean values of two groups was tested by Student's *t* test. The Kolmogorov-Smirnov test (see Fig. 5) was performed using software written in Igor. A probability of $P \leq 0.05$ was considered significant.

RESULTS

Quantal Events Resemble Those of Excitable Cells

We begin by describing the amperometric signature of exocytosis in epithelial cells for comparison with better-characterized systems. Touching a polarized carbon-fiber electrode gently to a single cell previously loaded in 70 mM dopamine or serotonin revealed spontaneous amperometric current spikes (Fig. 1, A and B). They reflect rapid oxidation of many thousands of oxidizable molecules released abruptly at the cell surface. In tests on five different batches of cells, signals were not observed without preloading the amine, indicating that the spikes represented the exogenous oxidizable amine. It was necessary to incubate epithelial cells in the 70-mM loading medium for longer than 30 min to detect the oxidation currents. Attempting to load with 1.5 mM of dopamine or serotonin for 4 h elicited much smaller peaks (not shown). Rates of spontaneous exocytosis ranged from 2 to 53 events per min (mean: 17.2 ± 4.9 events/min, $n = 11$ cells). The rate typically decreased over 4–5 h after loading was stopped, presumably due to a loss of vesicular amines through spontaneous exocytosis and by leak of cytoplasmic amines to the culture medium.

As shown in Fig. 1 B, each spike had the rapid onset and decay that are characteristic of exocytotic release from single secretory vesicles in other systems (Wightman et al., 1995). To analyze the kinetics of single events, amperometric recordings were filtered at 500 Hz frequency (−3 dB cut off). The average half-width of events was 5.0 ± 0.3 ms (118 events from 10 experiments). The average 10–90% rise and fall times were 1.13 ± 0.06 and 6.7 ± 0.3 ms, respectively. As the measured 10–90% rise time of a square pulse filtered the same way was 0.70 ms, the true rise time of amperometric events should be much shorter than the measured value. The short overall time course of the events is consistent with a diffusion distance of <1 μm between the amperometric probe and sites of release (Chow and von Rüden, 1995).

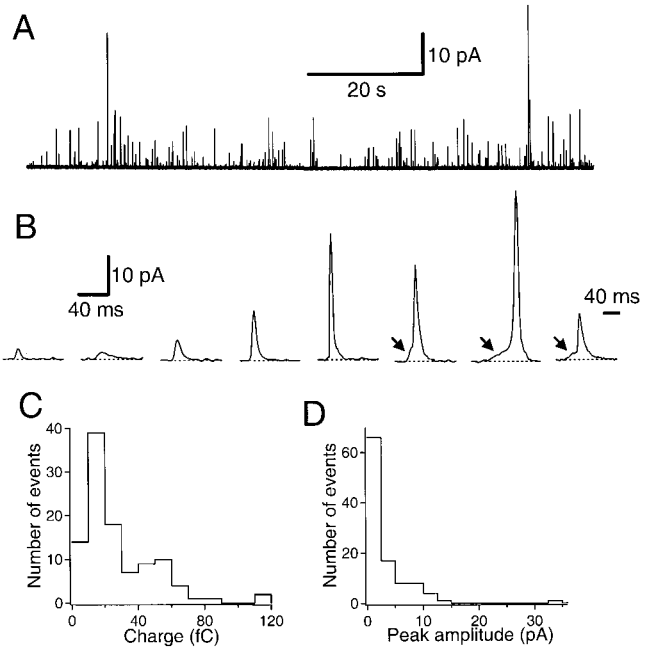

FIGURE 1. Quantal secretory events detected in a dog pancreatic duct epithelial cell. (A) Representative amperometric signals. The cell was loaded in 70 mM serotonin solution and exocytotic events were monitored with a carbon-fiber electrode polarized at +600 mV in serotonin-free solution. (B) Quantal events from the same experiment plotted at higher time resolution. The arrows indicate "feet" preceding main spikes. The last event on the right is plotted on a different time scale. (C) Charge distribution histogram from the same experiment. Integrals of 105 individual amperometric spikes acquired without stimulation were analyzed. (D) Peak amplitude histogram of the same recording. Filter frequency: 200 Hz.

Preceding large events with a good signal-to-noise ratio (Fig. 1 B), one could occasionally see a small step of release preceding the main event, named the "foot" by Chow et al. (1992). In chromaffin cells and mast cells, the foot current represents leakage of the secretory product through a flickering fusion pore before full dilation of the structure connecting a vesicle to the plasma membrane (Alvarez de Toledo et al., 1993; Zhou et al., 1996). The charge and peak amplitude distribution histograms of single amperometric events were broad, with respective means of 30.3 fC and 0.7 pA in this particular experiment using a serotonin-loaded cell (Fig. 1, C and D). The peak amplitude of amperometric events from cells loaded with 70 mM dopamine or serotonin varied from <1 pA to several tens of picoamperes (mean amplitude in nine cells, 0.93 ± 0.11 pA, at a filter frequency of 100 Hz). The time integral of the current in single events had a mean charge of 16.5 ± 2.5 fC ($n = 15$ cells) or ~103,000 electronic charges per event. For a two-electron oxidation of dopamine, this would correspond to ~51,500 molecules per spike. The similarities with amperometric studies in other cells argue that these amperometric spikes represent quantal exocytosis of loaded amines and that release begins with

formation of a fusion pore (see DISCUSSION). However, one difference here is the extreme range of sizes of the amperometric events. Since our loading and recording methods did not isolate a specific class of secretory vesicles (Kim et al., 2000), the broad range of event sizes detected probably reflected various degrees of filling of exocytotic vesicles of varying sizes.

Ca^{2+} Stimulates Exocytosis

As for neurons and many endocrine cells, exocytosis in the pancreatic duct epithelial cells could be stimulated by elevating $[Ca^{2+}]_i$. We used the Ca^{2+} ionophore, ionomycin, to bring Ca^{2+} into the cytoplasm. Dopamine-loaded cells were incubated in Ca^{2+}-free solution containing 5 μM ionomycin for 5–10 min. Subsequent application of a solution containing 2 mM Ca^{2+} induced vigorous exocytosis (Fig. 2, A and B). The significant rise of the current baseline during the Ca^{2+} application very likely reflected spillover of released dopamine from regions not directly under the electrode—on the same cell and on neighboring cells. The mean rate of exocytosis increased to 9.6 ± 2.4 (n = 16) times the control rates. The barrage of exocytotic events seen at the end of the Ca^{2+} application in Fig. 2 A was not seen in other similar experiments. It may reflect the sudden rise of $[Ca^{2+}]_i$ late in the Ca^{2+} application (Fig. 2 C).

We wanted to estimate the dependence of exocytosis on the mean $[Ca^{2+}]_i$ achieved with ionomycin treatment. Initial experiments with indo-1 had shown that application of 2 mM Ca^{2+} in the presence of ionomycin raised $[Ca^{2+}]_i$ into the range where the response of indo-1 saturates. Therefore, we switched to mag-indo-1-AM, a dye with much lower Ca^{2+} affinity. In various cells exposed to 2 mM Ca^{2+}, $[Ca^{2+}]_i$ increased monotonically, after a delay of ~1 min (Fig. 2, C and D). The average $[Ca^{2+}]_i$ reported by this dye at the end of the 3-min Ca^{2+} stimulation was 313 ± 74 μM (n = 8). Although $[Ca^{2+}]_i$ rose for several minutes, exocytosis developed early, before a large change in the mag-indo-1 signal was observed, indicating that exocytosis can be efficiently induced at low micromolar concentrations of Ca^{2+} (Fig. 2 D). To improve our estimate, we examined exocytosis in ionomycin with several lower Ca^{2+} concentrations in the bathing solution (Fig. 3, A and B). The 1 mM Ca^{2+} was about as effective as 2 mM, and 300 μM elicited a half-maximal rate of exocytosis. After these 3-min incubations in 5 μM ionomycin, the $[Ca^{2+}]_i$ was definitely not proportional to extracellular $[Ca^{2+}]$. With 1 mM Ca^{2+} outside, the $[Ca^{2+}]_i$ rose to 107 ± 25 μM (n = 9), whereas with 300 and 100 μM outside, it reached only 419 ± 41 nM (n = 5) and 176 ± 13 nM (n = 6), respectively. (The first value was measured with mag-indo-1 and the latter two with indo-1.) Apparently, cellular Ca^{2+} clearance mechanisms remained relatively effective with the lower bath $[Ca^{2+}]$,

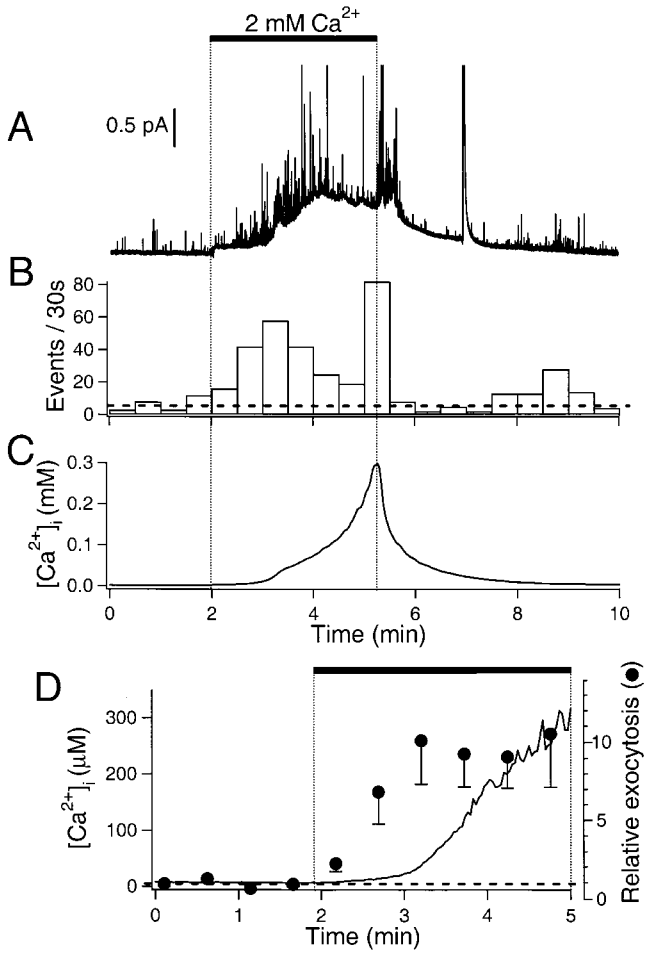

FIGURE 2. Stimulation of exocytosis by Ca^{2+} entry. (A) Amperometric record. Dopamine-loaded cells were treated with 5 μM ionomycin in Ca^{2+}-free external saline solution containing 100 μM EGTA for >6 min before the recording. External solution containing 2 mM Ca^{2+} was applied as indicated by the bar. Ionomycin was present throughout the recording. The large deflection near 7 min may represent breakdown of a nearby cell releasing a large quantity of dopamine into the medium. (B) Rate of exocytosis for the recording in A. The horizontal broken line indicates average rate of exocytosis in the control period. (C) Simultaneous Ca^{2+} measurement from the same cell using a low-affinity Ca^{2+} dye, mag-indo 1-AM. (D) Averaged kinetics of Ca^{2+} rise and exocytosis for many cells. $[Ca^{2+}]_i$ (n = 8, line) and relative rate of exocytosis (n = 16, ●) measured as 2 mM Ca^{2+} was applied to cells (horizontal bar). Basal $[Ca^{2+}]_i$ and the normalized rate of exocytosis (1.0) in the control period are indicated by a horizontal broken line. Error bars are shown only in the downward direction.

and they seemed to become overwhelmed if $[Ca^{2+}]_i$ rose above 5 μM for many seconds. This result led us to use higher concentrations of ionomycin, longer incubations, and Ca^{2+} clearance inhibitors when calibrating the dyes (see METHODS). In any case, exocytosis from the pancreatic epithelial cells is quite sensitive to Ca^{2+} since it reaches significant levels already with $[Ca^{2+}]_i$ as low as 300–400 nM (Fig. 3 C).

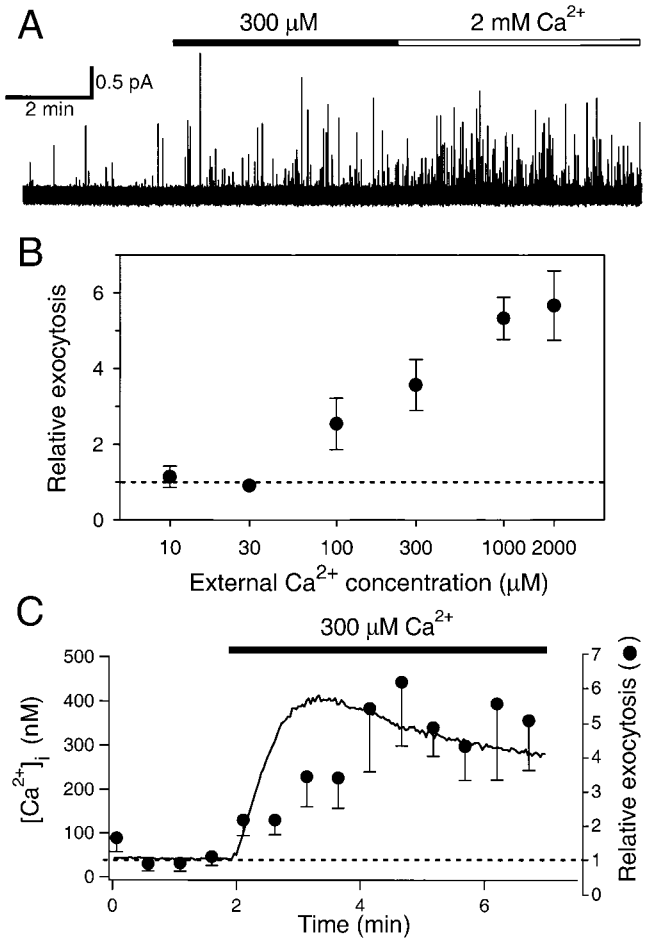

FIGURE 3. Exocytosis induced by $[Ca^{2+}]_i$. (A) Amperometric record acquired in an ionomycin-pretreated cell as in Fig. 2 A. Solutions containing 300 μM (closed bar) or 2 mM Ca^{2+} (open bar) were applied as indicated. (B) Rate of exocytosis in the presence of solutions containing different added Ca^{2+} was averaged for 6-min recording time and compared with that in control (3–14 cells per data point). (C) Average time course of $[Ca^{2+}]_i$ rise and exocytosis for several cells treated with ionomycin. Basal measurements were made in Ca^{2+}-free external solution and then cells were treated with solutions containing 300 μM Ca^{2+}. Intracellular $[Ca^{2+}]_i$ was measured with the high-affinity dye, indo-1 AM ($n = 5$), and relative rate of exocytosis was averaged from 12 cells.

Other Signaling Systems Elevate $[Ca^{2+}]_i$

Secretion from many gastrointestinal and airway epithelia can be stimulated by hormones and drugs that elevate intracellular levels of cAMP or stimulate phospholipase C. In cultured dog pancreatic epithelial cells, mucin secretion is induced by treatments that elevate cAMP (Oda et al., 1996). We therefore determined whether the exocytosis detected by amperometry is similarly enhanced. However, to establish whether any stimulation observed was secondary to an elevation of $[Ca^{2+}]_i$, we first monitored $[Ca^{2+}]_i$ using indo-1 as an indicator (Table I). The conditions tested included addition of forskolin, a direct activator of adenylyl cyclase, of epinephrine or VIP, whose receptors activate adenylyl cyclase (Oda et al., 1996), and of membrane-permeant 8-Br-cAMP. Each treatment often induced a modest transient elevation of $[Ca^{2+}]_i$, although not always. Therefore, in the following two sections, when asking if there is a Ca^{2+}-independent component of exocytosis with these treatments, we buffered changes of $[Ca^{2+}]_i$ by preincubating cells for 1 h in 50 μM BAPTA-AM, the membrane-permeant form of the Ca^{2+} chelator BAPTA (Table I).

cAMP Induces PKA-dependent and $[Ca^{2+}]_i$-independent Exocytosis

Fig. 4 A illustrates a typical long-lasting amperometric recording before and after activation of adenylyl cyclase by forskolin in a BAPTA-loaded cell. After 3 min of control recording, 20 μM forskolin was applied and the frequency of amperometric spikes gradually increased. The number of events in every 30-s interval is plotted in Fig. 4 B. The frequency rose from near 6/min in control to 32/min after forskolin treatment, a fivefold increase. The activation was first apparent at 30–60 s, and grew even after the forskolin was removed. The simultaneous $[Ca^{2+}]_i$ measurement (Fig. 4 C) confirmed that preloading with BAPTA had effectively eliminated any $[Ca^{2+}]_i$ transient during the forskolin treatment.

The time course of individual quantal events was not changed by forskolin treatment. Thus, the average half-width of events was 4.9 ± 0.2 ms (204 events from 10 experiments, at a filter frequency of 500 Hz; $P = 0.89$ compared with the value of control events). The average 10–90% rise- and fall-times were 1.13 ± 0.04 and 6.7 ± 0.3 ms, respectively. The mean current amplitude and charge of quantal events were slightly increased by forskolin treatment (1.11 ± 0.07 pA ($P = 0.04$) and 17.9 ± 2.1 fC ($P = 0.39$), respectively, $n = 15$ cells). Forskolin increased the rate of release of quanta of all sizes, but selectively enhanced the release of larger quanta, as can be seen in the histograms of Fig. 5 that compare the fraction of events in each charge range. (A significance of $P = 0.002$ was calculated with the Kolmogorov-Smirnov test using a cumulative histogram of the same data.)

The effects of forskolin on cells with and without BAPTA loading are summarized in Fig. 6 A. The amperometrically detected exocytosis rate in forskolin was 3.4 ± 1.2 ($n = 8$) relative to controls in BAPTA-loaded cells and 3.4 ± 0.6 ($n = 23$) in BAPTA-free cells. The basically identical effects of forskolin with or without buffering of the small transient rise of $[Ca^{2+}]_i$ (Table I) indicated that forskolin-stimulated exocytosis was mainly activated by cAMP. In parallel, we tested other agents known to increase intracellular cAMP levels and mucin secretion in these pancreatic epithelial cells (Oda et al., 1996). As anticipated, the amperometrically detected

TABLE I

$[Ca^{2+}]_i$ Elevations during Different Treatments

Agent	Without BAPTA loading		After BAPTA loading	
	nM	*n*	*nM*	*n*
Forskolin	92 ± 25	11	5.5 ± 3.2	5
Epinephrine	1045 ± 283	7	ND	
VIP	82 ± 38	4	ND	
8-Br-cAMP	447 ± 257	4	ND	
PMA	33 ± 23	4	5.3 ± 7.1	4

$[Ca^{2+}]_i$ was measured in indo-1-AM–loaded cells. Resting $[Ca^{2+}]_i$ was on average 67 ± 3 nM (n = 30). Peak $[Ca^{2+}]_i$ was measured during forskolin (20 μM), epinephrine (1 μM), VIP (1 μM), 8-Br-cAMP (1 mM), or PMA (100 nM) treatments. Increase in $[Ca^{2+}]_i$ above the resting levels after the treatment was analyzed.

exocytosis rates were increased by 1 μM epinephrine (5.1 ± 1.1, n = 8), 1 μM VIP (4.4 ± 2.0, n = 4), and 1 mM 8-Br-cAMP (4.0 ± 0.9, n = 7) (Fig. 6 A). In these experiments, cells were not loaded with BAPTA, so some of the increase of exocytosis with epinephrine and 8-Br-cAMP could have been due to a $[Ca^{2+}]_i$ rise in addition to their cAMP effect.

Does the stimulation of exocytosis require activation of cAMP-dependent protein kinase (PKA)? As a test, we compared the actions of the Rp and Sp enantiomers of 8-Br-cAMPS (Fig. 6 B). The Rp isomer is a specific inhibitor of PKA, and the Sp isomer is an activator. Application of Rp-8-Br-cAMPS did not change the rate of exocytosis in unstimulated cells (1.06 ± 0.15, n = 6), but it blocked the effect of forskolin applied 5 min later (0.80 ± 0.11, n = 6). In contrast, application of Sp-8-Br-cAMPS increased exocytosis by itself (2.7 ± 0.3, n = 9). These actions further support the hypothesis that stimulation of exocytosis is mediated through cAMP and PKA.

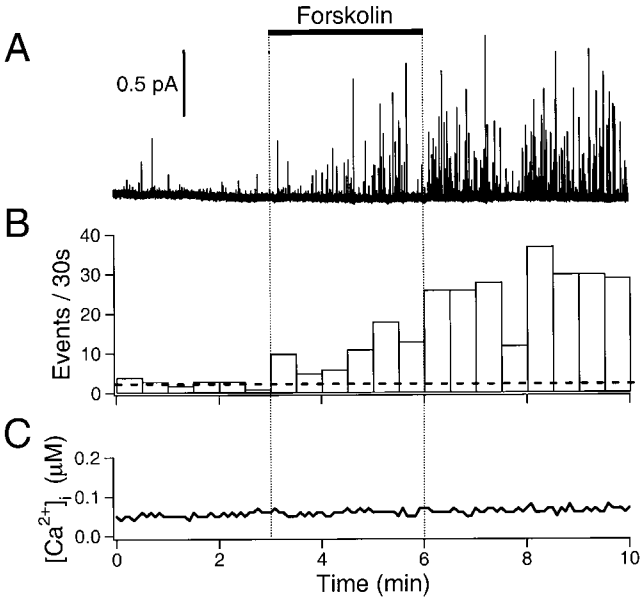

FIGURE 4. Ca^{2+}-independent increase of exocytosis with forskolin. (A) Amperometric record. The cell was incubated with 50 μM of BAPTA-AM for 1 h before loading with dopamine and indo 1-AM. Forskolin (20 μM) was applied to the cell for 3 min (bar). (B) Rate of exocytosis for the recording in A. The horizontal broken line indicates the average rate of exocytosis in the control period. (C) Simultaneous ratiometric Ca^{2+} measurement using indo-1. All data are from a single cell.

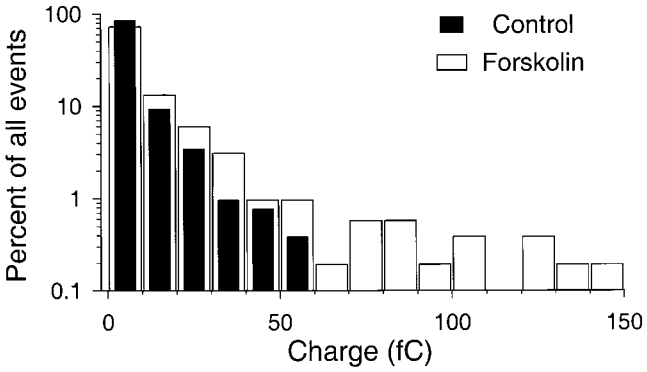

FIGURE 5. Charge distributions of amperometric events in control and forskolin. Amperometric events were pooled from six consecutive experiments using the same electrode. To acquire enough events, cells were recorded for 5–10 min in control before the 5-min forskolin (20 μM) treatment. For forskolin, the 2-min analysis period started after 2 min and the mean rate was about 2.5× that in the control. 518 events larger than 1 fC were analyzed for each histogram. The smallest bars are single events.

PKC also Stimulates $[Ca^{2+}]_i$-independent Exocytosis

We then tested the phorbol ester PMA to ask whether activating PKC also increased amperometrically detected exocytosis. The elevation of $[Ca^{2+}]_i$ by PMA is minimal (Table I). Nevertheless, we preloaded one batch of cells with BAPTA and tested the actions of 100 nM PMA. The phorbol ester increased exocytosis (Fig. 7, A and B) without any accompanying change of $[Ca^{2+}]_i$ (Fig. 7 C; and Table I), but the potentiation of exocytosis was smaller than that by cAMP. On average, this concentration of PMA elevated relative exocytosis to 2.7 ± 0.6 (n = 5) in cells preloaded with BAPTA and to 2.4 ± 0.4 (n = 13) without BAPTA (Fig. 8 A). These values are not statistically different (P = 0.67). Next, we did controls to check whether PMA acted via PKC to increase exocytosis. A structurally related but inactive compound, 4-α-phorbol-12,13-didecanoate (4-α-phorbol) slightly increased exocytosis (1.37 ± 0.27, n = 5) at a concentration of 100 nM; this increase, however, was not statistically significant (P = 0.12). To reduce possible nonspecific effects, the concentration of the active and control phorbol esters was decreased to 10 nM (Fig. 8 B). Exocytosis was still significantly evoked by PMA at 10 nM (2.2 ± 0.4, n = 4) but not by 4-α-phorbol (0.95 ± 0.21, n = 4). The PKC-selective inhibitor, BIS (500 nM), slightly reduced exocytosis by itself (0.68 ± 0.07, n = 10). After a 5-min incubation with

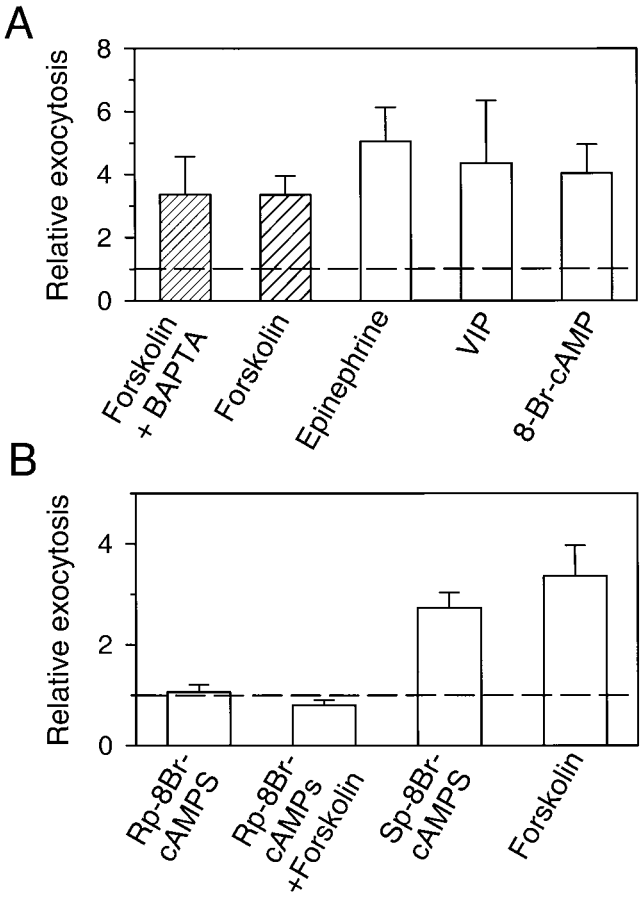

FIGURE 6. Regulation of exocytosis by cAMP and PKA. (A) Stimulation by different agents known to raise intracellular cAMP. Cells were treated with forskolin (20 μM), epinephrine (1 μM), VIP (1 μM), or 8-Br-cAMP (1 mM) for 3 min. Relative exocytosis is the ratio of exocytosis after and before the treatment. One group of cells (Forskolin + BAPTA) was pretreated with 50 μM BAPTA-AM for 1 h. (B) Evidence that PKA is needed. After the rate of exocytosis was measured in control saline solution, the PKA-specific inhibitor, Rp-8-Br-cAMPS, was applied to the bath for 5 min at an estimated final concentration of 2 mM. The rate of exocytosis in Rp-8Br-cAMPS was measured during the last 2 min of application of the inhibitor. Then, forskolin (~20 μM) was added to the bath (Rp-8Br-cAMPS + Forskolin). In both cases, the rate of exocytosis was compared with that in control condition. With other sets of cells, the PKA-specific activator, Sp-8-Br-cAMPS, was applied to bath (Sp-8Br-cAMPS, ~2 mM). The value for forskolin alone is same as in A. Cells were loaded with either dopamine or serotonin.

BIS, PMA was not able to evoke exocytosis (0.44 ± 0.07, $n = 9$). The further decrease of exocytosis during the combined application of BIS and PMA may be due to a continued slow development of the effect of BIS.

With PKA and PKC Blocked, Exocytosis Is Induced Only by High $[Ca^{2+}]_i$

Using simultaneous measurements of $[Ca^{2+}]_i$ and exocytosis, we have demonstrated that PKA and PKC can increase exocytosis when $[Ca^{2+}]_i$ rises are blocked with BAPTA. Now we asked if the reverse is true. Can Ca^{2+}

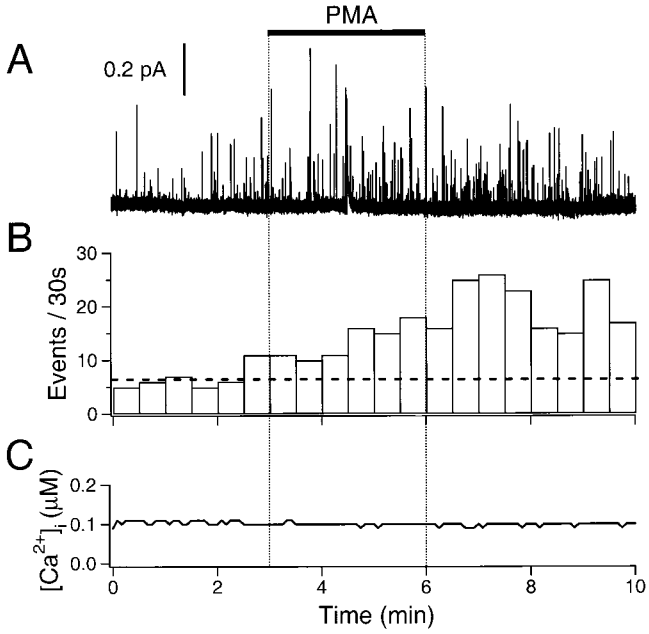

FIGURE 7. Stimulation of exocytosis by PMA. (A) Amperometric record. The cell was preincubated in 50 μM BAPTA-AM for 1 h, and then loaded with dopamine and indo 1-AM. PMA (100 nM) was applied for 3 min as indicated by the bar. (B) The rate of exocytosis for the same cell. The horizontal broken line indicates the average rate of exocytosis in the control period. (C) Simultaneous Ca^{2+} measurement using indo-1 dye in the same cell.

induce exocytosis when protein kinases are blocked? In these experiments, we use BIS to block PKC as before, and H-89 to block PKA. (The expense of using Rp-8-Br-cAMPS would have been too great.) To check the efficacy of H-89 in blocking PKA, we asked whether pretreatment with 10 μM H-89 for 5 min reduced relative exocytosis induced by 10 μM forskolin. In untreated cells, forskolin raised relative exocytosis from 3.31 ± 0.85 ($n = 3$), and in H-89–treated cells, forskolin was ineffectual (1.15 ± 0.22, $n = 7$, relative to H-89 alone).

Both kinase inhibitors depressed relative exocytosis in control experiments. It was reduced to 0.64 ± 0.05 by H-89 ($n = 27$) and to 0.76 ± 0.06 ($n = 24$) by BIS (Fig. 9 A). The depression implies either that there is some background activation of the kinases in unstimulated cells or that the inhibitors have nonspecific actions at other steps in exocytosis. Therefore, in the statistical tests below, we use the H-89- or BIS-inhibited measurement as the control value for calculating the effect of subsequently added Ca^{2+}.

Next, tests were done on the effects of $[Ca^{2+}]_i$ elevation while kinases were inhibited. The first tests used 300 μM extracellular Ca^{2+}, which raises $[Ca^{2+}]_i$ only to submicromolar concentrations (~400 nM). The low Ca^{2+} stimulus applied to uninhibited, ionomycin-treated cells increased relative exocytosis to 3.01 ± 0.37 (Fig. 9 A). The same stimulus was not effectual on cells treated with 10 μM H-89 (0.71 ± 0.21, $n = 8$, relative exocytosis

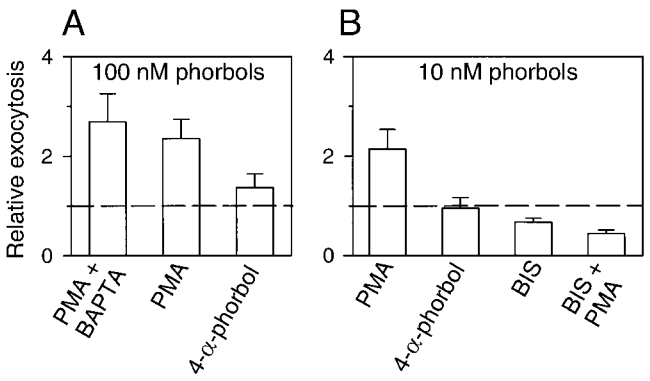

FIGURE 8. PMA acts by stimulating PKC. (A) Relative exocytosis during 3-min treatments with PMA (100 nM) or its structurally related inactive analogue, 4-α-phorbol (100 nM). Some cells (PMA + BAPTA) were preincubated with 50 μM of BAPTA-AM for 1 h. (B) Same treatments as in A, but with a lower concentration (10 nM) of PMA or 4-α-phorbol. Some cells were treated with the PKC inhibitor, BIS (500 nM). The rate of exocytosis in BIS was measured during the last 2 min of the 5-min application of the inhibitor. In both cases, the rate of exocytosis was compared with that in control condition. Then, PMA (10 nM) was added (BIS + PMA). Cells were loaded with dopamine.

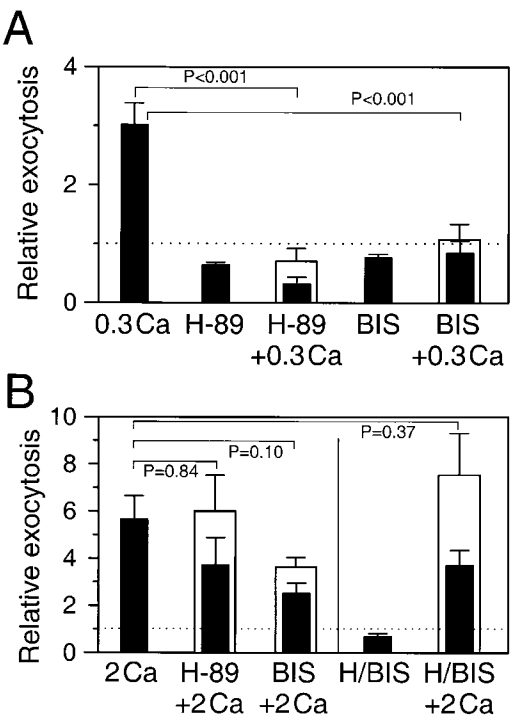

FIGURE 9. Possible role of protein kinases in Ca^{2+}-induced exocytosis. Bars represent relative exocytosis compared with either untreated control recording (closed bars) or recording obtained with the inhibitors H-89 or BIS (open bars). All statistical tests compare the data in the open bars with calcium treatments in uninhibited cells. (A) Exocytosis induced by small $[Ca^{2+}]_i$ elevations. Relative rates of exocytosis induced by 300 μM Ca^{2+} alone (0.3Ca), or after incubation for 5 min with 10 μM H-89 (H-89), H-89 with 300 μM Ca^{2+} (H-89 + 0.3Ca), 500 nM BIS (BIS), or BIS with 300 μM Ca^{2+} (BIS + 0.3Ca). (B) Exocytosis induced by higher $[Ca^{2+}]_i$. Relative rates of exocytosis with 2 mM Ca^{2+} alone (2Ca), H-89 with 2 mM Ca^{2+} (H-89 + 2Ca), BIS with 2 mM Ca^{2+} (BIS + 2Ca), combined treatments of H-89 and BIS (H/BIS), or H-89 and BIS with 2 mM Ca^{2+} (H/BIS + 2Ca). The rate of exocytosis was measured for 3 min in controls and 5 min for inhibitors or inhibitors with Ca^{2+}. Cells were loaded with dopamine.

compared with H-89 alone) or with 500 nM BIS (1.08 ± 0.26, n = 16, relative exocytosis compared with BIS alone). Thus, protein kinase inhibitors block the effects of small $[Ca^{2+}]_i$ elevations. Then tests were repeated with 2 mM extracellular Ca^{2+}, which raises $[Ca^{2+}]_i$ to 300 μM. The exocytosis induced by this stimulus was not significantly reduced by inhibition of PKA or PKC or by simultaneous inhibition of both kinases (Fig. 9 B).

Some Properties of Exocytosis Differ Between Epithelial and Excitable Cells

In the beginning of the RESULTS, we emphasized similarities between the secretion in epithelial cells and that of excitable cells. There are some clear differences, however: insensitivity to hypertonic shocks, insensitivity to KCl depolarization, and occasional giant multi-vesicular secretory events.

Synapses release a small number of neurotransmitter quanta upon sudden stimulation with hypertonic solutions (Furshpan, 1956; Rosenmund and Stevens, 1996), and such stimuli are considered a reliable way to assay the size of the "readily releasable pool" of docked and primed neurotransmitter vesicles. In contrast, a saline solution supplemented with 250 mM sucrose strongly decreased the relative rate of amperometric events from our epithelial cells (Fig. 10, to 0.28 ± 0.08, n = 12). There was no apparent change of cell volume or visible detachment of the carbon electrode from the cell, and the effect of hypertonic solution was reversible (1.05 ± 0.18, n = 10).

In excitable cells, exocytosis is normally stimulated by membrane depolarization, which allows Ca^{2+} to enter cells via voltage-gated Ca^{2+} channels. As exocytosis from epithelial cells is also Ca^{2+} sensitive, it was interesting to test whether they can use a voltage-gated Ca^{2+} influx mechanism. The resting potential of the cultured epithelial cells was relatively low, −39 ± 2.1 mV (measured under perforated-patch conditions). It depolarized to −21 ± 3.1 mV (n = 11) when all the extracellular NaCl was replaced by KCl. However, the KCl depolarization did not change the rate of exocytosis (exocytosis relative to control = 0.97 ± 0.07, n = 9), indicating that, at least in this potential range, these cells lack voltage-gated Ca^{2+} entry mechanisms.

We occasionally observed large, long-lasting amperometric events. These complex events were characterized by multiple overlapping peaks, suggesting compound exocytosis with overlapping fusion of a large number of vesicles (Fig. 11). As an empirical criterion to detect

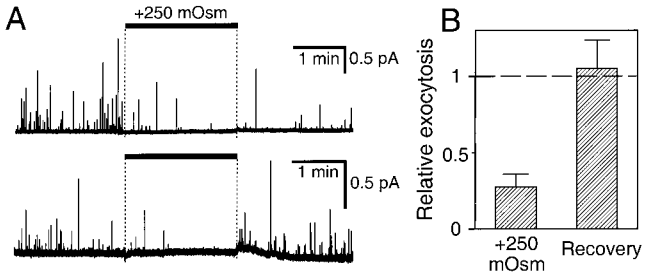

FIGURE 10. Depression of exocytosis by hyperosmotic solution. (A) Amperometric recordings from two cells loaded with dopamine. Cells were treated with external saline solution supplemented with 250 mOsm sucrose for 2 min (bar). (B) Summary of results of 12 experiments normalized to the initial control period.

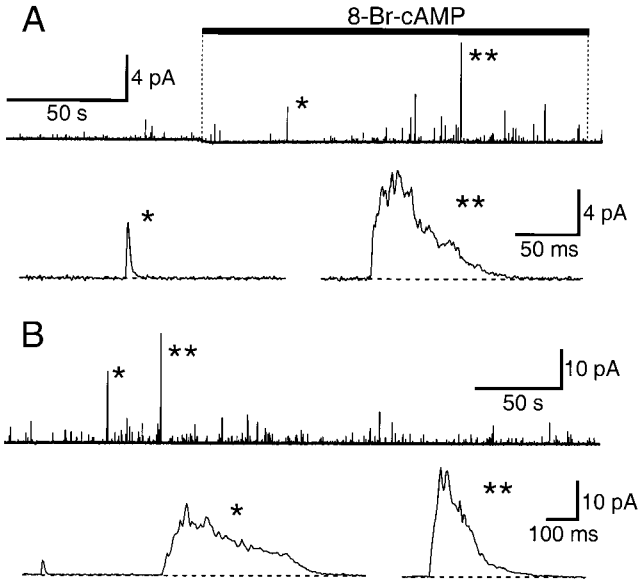

FIGURE 11. (A) Complex exocytosis. Amperometric recording from a cell loaded with dopamine. Cells were treated with 1 mM 8-Br-cAMP as indicated by a bar. A quantal event (*) and a large and long-lasting complex event (**) are shown on an expanded time scale. The complex event contained 131× more charge than the average quantal events in this recording. One complex event was observed in 109 quantal events in this experiment. Filter frequency: 200 Hz. (B) A similar experiment to A. The cell was treated with thapsigargin 10 min before the start of recording. The marked events contained 130 (*) and 101 (**) times more charge than the average quantal event in the recording. Two complex events were observed in 538 quantal events in this experiment. Filter frequency: 100 Hz.

such events, we used a sliding window of 50 adjacent sample points. A large event was scored if the total charge in this interval exceeded 20× the average charge of a single quantal event. The window was moved by 25 points each time to ensure the detection of the complex events. By this criterion, there were 12 giant events out of 2,714 amperometric events (one per 226 events) in seven experiments. The occurrence may be overestimated, as only recordings containing at least one obvious complex event were included in this analysis. The average charge of such complex amperometric events was 99 ± 25 (n = 7) times that of the quantal events. Such events were seen both during stimulated release and during spontaneous release in unstimulated cells.

DISCUSSION

Secretion in Epithelia

The physiological ion transport and exocytosis in epithelia are regulated by hormones and neurotransmitters through stimulation of either adenylyl cyclase or phospholipase C. In most studies, it has not been possible to measure or regulate possible intracellular Ca^{2+} transients in response to the hormones. For hormones acting via phospholipase C, a Ca^{2+} transient as well as activation of PKC would be expected; all these pathways stimulate mucin secretion (Forstner et al., 1993; Davis and Abdullah, 1997).

Secretion of mucin has previously been demonstrated in confluent monolayers of the cultured dog pancreatic epithelial cells used here. VIP and epinephrine raised the cAMP content of these differentiated cells approximately sixfold, and 4-h incubations with VIP, epinephrine, or dibutyryl cAMP increased mucin secretion to 1.5–3× control amounts (Oda et al., 1996). Similarly, treatment with ATP, which activates $P2Y_2$ purinergic receptors in these cells and stimulates phospholipase C, generated a $[Ca^{2+}]_i$ transient, and increased mucin secretion approximately fourfold (Nguyen et al., 1998). Calcium elevations alone, achieved with the ionophore A23187, stimulated mucin secretion threefold. Using single-cell biophysical methods, we have now shown that activation of PKA or PKC evoked Ca^{2+}-independent exocytosis from nonconfluent monolayers of the same cells. A variety of stimuli increased exocytosis within 1–3 min. In our work, secretion rose to three to five times the control rate after cAMP stimuli (Figs. 4 and 6), two to three times after PMA (Figs. 7 and 8), and nine times after ionomycin (Fig. 2). Thus, the determinants of exocytosis assessed by amperometric measurements are comparable with the previously reported direct measurement of mucin secretion.

We provide further evidence that stimulation by cAMP requires activation of PKA and does not require a $[Ca^{2+}]_i$ elevation, and that PKC also will stimulate exocytosis without a $[Ca^{2+}]_i$ elevation. Finally, high levels of $[Ca^{2+}]_i$ alone can evoke exocytosis without activation of PKA or PKC. However, exocytosis evoked by submicromolar Ca^{2+} was significantly reduced when the protein kinases are pharmacologically inhibited. Such results suggest that Ca^{2+} induces exocytosis by different pathways depending on its concentration, but a definitive conclusion awaits further study with other types of protein kinase inhibitors or cells lacking PKA or PKC expression.

Comparison of Epithelia and Excitable Cells

The secretory mechanisms of excitable cells and epithelia have similarities and differences. Our study may be the first to apply amperometry to epithelial secretion. This allows an improvement of the time resolution of several orders of magnitude and resolution of single-vesicle release events. As in excitable cells, we find that the basic release event has a rise time shorter than 1 ms and is preceded, for some events, by a foot lasting several milliseconds. It appears, therefore, that, as in mast cells or chromaffin cells (Breckenridge and Almers, 1987; Chow et al., 1992), the secretory vesicle passes through a transient phase with potentially reversible formation of a stereotyped fusion pore, which has a variable lifetime followed by sudden dilatation that allows maximal release of the vesicle contents. The amperometric spikes are relatively brief, having a falling time constant of ~7 ms and half widths of 5 ms. This lies between the observed 5–15-ms half widths for catecholamine release from mammalian chromaffin cells (Wightman et al., 1995) and the 0.6- and 3.7-ms half widths of two classes of serotonin release from a leech synapse (Bruns and Jahn, 1995).

What are the differences from excitable cells? As they apparently lack voltage-gated calcium channels, depolarization does not stimulate exocytosis in epithelial cells as it does in excitable cells. Additionally, hypertonic solutions depress exocytosis in our cells and in chromaffin cells (Holz and Senter, 1986), unlike in neuronal synapses (Furshpan, 1956; Rosenmund and Stevens, 1996). Finally, the apparent speed of regulation of exocytosis seems much less than in a synapse. The effects of the stimuli take at least tens of seconds to develop in epithelia. In contrast, in a synapse, the rate of release can increase 1,000-fold during an action potential (Barrett and Stevens, 1972; Goda and Stevens, 1994), and the full stimulation rises and falls within <1 ms. This difference may suggest a completely different Ca^{2+} sensor acting at a different point in the vesicle delivery pathway. Judging from the effects of protein kinase inhibitors, the resting secretion in epithelial cells may reflect a small basal stimulation of the cAMP and PKC pathways, as is found in other systems.

All of these functional differences may point to well-known structural factors. In epithelia, although many secretory granules may be near the plasma membrane (Oda et al., 1996), there is no known active zone and the fusion machinery is certainly not intimately attached to voltage-gated Ca^{2+} channels as at a synapse. Even in chromaffin cells, where there are Ca^{2+} channels, a significant fraction of docked vesicles may not be in close proximity (Chow et al., 1992; Voets et al., 1999). It is possible that, unlike in synapses, epithelial secretion is not based on a pool of primed vesicles requiring only <1 ms for final fusion. There may remain many constitutive biochemical steps that separate the actions of kinases from the fusion events they ultimately accelerate. Also in epithelia and chromaffin cells, the size of the typical secretory granule is 5–30× larger than a neurotransmitter vesicle of synapses, and the granules contain newly synthesized proteins. Hence, the vesicles must be formed differently and have some different components. Indeed, the proteins of the secretory machinery in nonneuronal cells are believed to be homologous but not always identical to members of the membrane and soluble protein families used in neurons. While the characterization of proteins involved in exocytosis in pancreatic duct cells is sparse, in pancreatic acinus, the other major exocrine cell type in pancreas, the proteins rab3D (Valentijn et al., 1996), syntaxin 2 (Hansen et al., 1999), and SNAP-23 (Gaisano et al., 1997) may serve the functions in apical secretion that are served by rab3A, syntaxin 1, and SNAP-25 in synaptic exocytosis. The protein syntaxin 3, which is associated with the acinar granules, may serve compound exocytosis, the intracellular fusion of granules to each other (Hansen et al., 1999). Many of the above proteins can be phosphorylated by various protein kinases, and their phosphorylation has been implicated in changes of exocytosis (Turner et al., 1999).

Protein-Kinase Sensitivity of Exocytosis in Neurons and Endocrine Cells

Ca^{2+} is very clearly the immediate trigger of evoked transmitter release at synapses. Nevertheless, pharmacological activation of PKA or PKC increases evoked and spontaneous excitatory and inhibitory postsynaptic currents two- to fourfold, much as in epithelial cells. For example, phorbol esters acting via PKC increase the frequency but not the amplitude of spontaneous GABA release from interneurons and glutamate release from hippocampal neurons (Finch and Jackson, 1990; Capogna et al. 1995). Activating PKA by forskolin has a similar effect on excitatory and inhibitory synapses (Chavez-Noriega and Stevens, 1994; Capogna et al., 1995). Phorbol esters also stimulate secretion in anterior pituitary cells (Billiard et al., 1997).

Which Vesicles Are Being Reported?

Our loading method does not allow selective study of a specific class of secretory vesicle in the way that a biochemical or postsynaptic current assay would. With the high serotonin and dopamine concentrations used here, loading does not depend on monoamine transporters (Kim et al., 2000). Instead, we believe that intracellular vesicles load passively with the exogenous monoamine if their lumen is acidic. Some of these vesicles may be components of constitutive membrane traffic. On average, the spontaneously released vesicles were smaller than the population released under cAMP stimulation. Never-

theless, the degree of stimulation of amperometric events by our treatments parallels the stimulation of mucin secretion measured directly in differentiated monolayers (Oda et al., 1996; Nguyen et al., 1998).

We can compare the number of oxidizable molecules released per quantum in different cells. In forskolin-stimulated pancreatic duct cells, we see a broad distribution of sizes and a mean of ~100,000 elementary charges, corresponding to ~50,000 dopamine molecules per vesicle, but with 20% of the events < 7,000 molecules and 7% > 100,000 molecules (Fig. 5). In the same kind of assay with cells containing endogenous catecholamine or serotonin, the approximate number of molecules released per quantum is 7×10^6 from chromaffin cells (Albillos et al., 1997), 35,000 from cultured sympathetic ganglion cells (Zhou and Misler, 1995), 40,000 and 800,000 from two vesicle populations in somata of the snail *Planorbis* (Chen et al., 1995), and 5,000 and 80,000 from two populations of vesicles in leech synapses (Bruns and Jahn, 1995). Should the larger amperometric events represent exocytosis of mucin granules, the dopamine concentration in these granule can be calculated to be 20 mM, assuming 100,000 dopamine molecules per granule and a granule diameter of 0.25 μm, as estimated from Oda et al. (1996). In chromaffin granules, the concentration of endogenously packaged catecholamine is near 700 mM (Albillos et al., 1997).

What are the giant complex events (Fig. 11)? The hypothesis that they represent the death of a cell, with release of all oxidizable contents, can be excluded by two observations. First, if the cell membrane is deliberately ruptured by advancing the amperometric probe by several micrometers, a much larger oxidation current (peak amplitude >50 pA) of longer duration (>10 s) was observed. This reflects a considerable quantity of cytoplasmic monoamine. Second, the more typical quantal events continue unabated with fast rise and fall times immediately after a complex event, suggesting that the cell is still functional and that its membrane remains within 1 μm of the probe.

A more likely explanation for these giant complex events is that a large number of quantal events are superimposed. This would account for the clear spike-like substructure of the complex event. However, it is unlikely that complex events are a random superposition of independent quantal events. We can estimate the chance of that occurring. Since the average frequency of spontaneous quantal events is one per 3 s, the probability of observing a quantum within a 500 ms time window is 1/6. Provided that amperometric events are randomly distributed, the probability of having 100 or more independent events occurring in a 500-ms time window is $\sim(1/6)^{100}$. The probability of seeing a complex event within 500 ms window was actually 1/1,360, calculated as the probability of observing any event (1/6) multiplied by fraction of complex events (1/226). Therefore, some concerted process must coordinate multivesicular events. It might be a form of compound exocytosis in which some vesicles are fusing to each other before the final fusion to the plasma membrane or it may represent a period in which the probability of fusion has been raised by several orders of magnitude by some intracellular signal. The number of molecules released in one giant event exceeds several million, which is comparable with the release from a typical chromaffin granule—except that it is spread out in time so that the amplitude is not 100× the mean quantal amplitude. Compound exocytosis and also apocrine-like secretion are commonly invoked in morphological studies of stimulated, mucin secreting epithelia (Phillips, 1992; Newman et al., 1996). Compound exocytosis has also been described in eosinophils (Scepek and Lindau, 1993). The unexpected finding is the large charge of these giant events and the scarcity of any events of charge intermediate between what we have called quantal and the giant events.

In conclusion, exocytosis in pancreatic duct epithelial cells shares several features with exocytosis in excitable cells. However, overall, the range of regulation, the speed of regulation, and the maximum rate of exocytosis are smaller. In the epithelium, the effects of kinases and Ca^{2+} are similar in magnitude, whereas in neurons the effect of Ca^{2+} is much stronger than that of kinases. Therefore, hormonal regulation via kinases becomes a viable way to regulate exocytosis from epithelia in the absence of any Ca^{2+} signal. Its molecular basis needs clarification.

We thank Drs. Ed Kaftan and Tao Xu for reading the manuscript and Drs. S.P. Lee and P. Verdugo for helpful discussions. We thank L. Miller and D. Anderson for technical assistance.

This work was supported by grants from the National Institutes of Health (AR17803), the Cystic Fibrosis Foundation (R565), and the Department of Veterans Affairs (Merit Review).

Submitted: 30 March 2000
Revised: 8 August 2000
Accepted: 9 August 2000

REFERENCES

Abdullah, L.H., J.D. Conway, J.A. Cohn, and C.W. Davis. 1997. Protein kinase C and Ca^{2+} activation of mucin secretion in airway goblet cells. *Am. J. Physiol. Cell Physiol.* 273:L201–L210.

Albillos, A., G. Dernick, H. Horstmann, W. Almers, G. Alvarez de Toledo, and M. Lindau. 1997. The exocytotic event in chromaffin cells revealed by patch amperometry. *Nature.* 389:509–512.

Almers, W., and E. Neher. 1987. Gradual and stepwise changes in the membrane capacitance of rat peritoneal mast cells. *J. Physiol.* 386:205–217.

Alvarez de Toledo, G., R. Fernandez-Chacon, and J.M. Fernandez. 1993. Release of secretory products during transient vesicle fusion. *Nature.* 363:554–558.

Barrett, E.F., and C.F. Stevens. 1972. The kinetics of transmitter release at the frog neuromuscular junction. *J. Physiol.* 227:691–708.

Billiard, J., D.-S. Koh, D.F. Babcock, and B. Hille. 1997. Protein kinase C as a signal for exocytosis. *Proc. Natl. Acad. Sci. USA.* 94: 12192–12197.

Breckenridge, L.J., and W. Almers. 1987. Currents through the fusion pore that forms during exocytosis of a secretory vesicle. *Nature.* 328:814–817.

Brown, D., T. Katsura, and C.E. Gustafson. 1998. Cellular mechanisms of aquaporin trafficking. *Am. J. Physiol. Renal Physiol.* 275: F328–F331.

Bruns, D., and R. Jahn. 1995. Real-time measurement of transmitter release from single synaptic vesicles. *Nature.* 377:62–65.

Capogna, M., B.H. Gähwiler, and S.M. Thompson. 1995. Presynaptic enhancement of inhibitory synaptic transmission by protein kinases A and C in the rat hippocampus in vitro. *J. Neurosci.* 15: 1249–1260.

Chavez-Noriega, L.E., and C.F. Stevens. 1994. Increased transmitter release at excitatory synapses produced by direct activation of adenylate cyclase in rat hippocampal slices. *J. Neurosci.* 14:310–317.

Chen, G., P.F. Gavin, G. Luo, and A.G. Ewing. 1995. Observation and quantitation of exocytosis from the cell body of a fully developed neuron in *Planorbis corneus*. *J. Neurosci.* 15:7747–7755.

Chow, R.H., and L. von Rüden. 1995. Electrochemical detection of secretion from single cells. *In* Single-Channel Recording. 2nd ed. B. Sakmann and E. Neher, editors. Plenum Publishing Corp., New York, NY, and London, UK. 245–275.

Chow, R.H., L. von Rüden, and E. Neher. 1992. Delay in vesicle fusion revealed by electrochemical monitoring of single secretory events in adrenal chromaffin cells. *Nature.* 356:60–63.

Coorssen, J.R., H. Schmitt, and W. Almers. 1996. Ca^{2+} triggers massive exocytosis in Chinese hamster ovary cells. *EMBO (Eur. Mol. Biol. Organ.) J.* 15:3787–3791.

Davis, C.W., and L.H. Abdullah. 1997. In vitro models for airways mucin secretion. *Pulm. Pharmacol. Ther.* 10:145–155.

Finch, D.M., and M.B. Jackson. 1990. Presynaptic enhancement of synaptic transmission in hippocampal cell cultures by phorbol esters. *Brain Res.* 518:269–273.

Forstner, G., Y. Zhang, D. McCool, and J. Forstner. 1993. Mucin secretion by T84 cells: stimulation by PKC, Ca^{2+}, and a protein kinase activated by Ca^{2+} ionophore. *Am. J. Physiol. Gastrointest. Liver Physiol.* 264:G1096–G1102.

Fujita-Yoshigaki, J. 1998. Divergence and convergence in regulated exocytosis: the characteristics of cAMP-dependent enzyme secretion of parotid salivary acinar cells. *Cell Signal.* 10:371–375.

Furshpan, E.J. 1956. The effects of osmotic pressure changes on the spontaneous activity at motor nerve endings. *J. Physiol.* 134: 689–697.

Gaisano, H.Y., L. Sheu, P.P. Wong, A. Klip, and W.S. Trimble. 1997. SNAP-23 is located in the basolateral plasma membrane of rat pancreatic acinar cells. *FEBS Lett.* 414:298–302.

Goda, Y., and C.F. Stevens. 1994. Two components of transmitter release at a central synapse. *Proc. Natl. Acad. Sci. USA.* 91:12942–12946.

Grynkiewicz, G., M. Poenie, and R.Y. Tsien. 1985. A new generation of Ca^{2+} indicators with greatly improved fluorescence properties. *J. Biol. Chem.* 260:3440–3450.

Hansen, N.J., W. Antonin, and J.M. Edwardson. 1999. Identification of SNAREs involved in regulated exocytosis in the pancreatic acinar cell. *J. Biol. Chem.* 274:22871–22876.

Hille, B., J. Billiard, D.F. Babcock, T. Nguyen, and D.-S. Koh, 1999. Stimulation of exocytosis without a calcium signal. *J. Physiol.* 520: 23–31.

Holz, R.W., and R.A. Senter. 1986. Effects of osmolality and ionic strength on secretion from adrenal chromaffin cells permeabilized with digitonin. *J. Neurochem.* 46:1835–1842.

Kawagoe, K.T., J.B. Zimmerman, and R.M. Wightman. 1993. Principles of voltammetry and microelectrode surface states. *J. Neurosci. Methods.* 48:225–240.

Kim, K.T., D.-S. Koh, and B. Hille. 2000. Loading of oxidizable transmitters into secretory vesicles permits carbon-fiber amperometry. *J. Neurosci.* 20:RC101,1–5.

Klinkspoor, J.H., G.N. Tytgat, S.P. Lee, and A.K. Groen. 1996. Mechanism of bile salt-induced mucin secretion by cultured dog gallbladder epithelial cells. *Biochem. J.* 316:873–877.

Koh, D.-S., and B. Hille. 1999. Rapid fabrication of plastic-insulated carbon-fiber electrodes for micro-amperometry. *J. Neurosci. Methods.* 88:83–91.

Koh, D.-S., M.W. Moody, T.D. Nguyen, B.L. Tempel, and B. Hille. 1997. Real-time detection of exocytosis in epithelial cells. *Soc. Neurosci. Abstr.* 22:467. (Abstr.)

Larivee, P., S.J. Levine, A. Martinez, T. Wu, C. Logun, and J.H. Shelhamer. 1994. Platelet-activating factor induces airway mucin release via activation of protein kinase C: evidence for translocation of protein kinase C to membranes. *Am. J. Respir. Cell. Mol. Biol.* 11:199–205.

Morimoto, T., S. Popov, K.M. Buckley, and M.M. Poo. 1995. Calcium-dependent transmitter secretion from fibroblasts: modulation by synaptotagmin I. *Neuron.* 15:689–696.

Neher, E., and W. Almers. 1986. Fast calcium transients in rat peritoneal mast cells are not sufficient to trigger exocytosis. *EMBO (Eur. Mol. Biol. Organ.) J.* 5:51–53.

Newman, T.M., A. Robichaud, and D.F. Rogers. 1996. Microanatomy of secretory granule release from guinea pig tracheal goblet cells. *Am. J. Respir. Cell. Mol. Biol.* 15:529–539.

Nguyen, T.D., C.N. Okolo, and M.W. Moody. 1998. Histamine stimulates ion transport by dog pancreatic duct epithelial cells through H1 receptors. *Am. J. Physiol. Gastrointest. Liver Physiol.* 275:G76–G84.

Oda, D., C.E. Savard, T.D. Nguyen, L. Eng, E.R. Swenson, and S.P. Lee. 1996. Dog pancreatic duct epithelial cells: long-term culture and characterization. A*m. J. Pathol.* 148:977–985.

Phillips, T.E. 1992. Both crypt and villus intestinal goblet cells secrete mucin in response to cholinergic stimulation. *Am. J. Physiol. Gastrointest. Liver Physiol.* 262:G327–G331.

Rosenmund, C., and C.F. Stevens. 1996. Definition of the readily releasable pool of vesicles at hippocampal synapses. *Neuron.* 16: 1197–1207.

Scepek, S., J.R. Coorssen, and M. Lindau. 1998. Fusion pore expansion in horse eosinophils is modulated by Ca^{2+} and protein kinase C via distinct mechanisms. *EMBO (Eur. Mol. Biol. Organ.) J.* 17:4340–4345.

Scepek, S., and M. Lindau. 1993. Focal exocytosis by eosinophils—compound exocytosis and cumulative fusion. *EMBO (Eur. Mol. Biol. Organ.) J.* 12:1811–1817.

Smith, P.A., M.R. Duchen, and F.M. Ashcroft. 1995. A fluorimetric and amperometric study of calcium and secretion in isolated mouse pancreatic β-cells. *Pflügers Arch.* 430:808–818.

Turner, K.M., R.D. Burgoyne, and A. Morgan. 1999. Protein phosphorylation and the regulation of synaptic membrane traffic. *Trends Neurosci.* 22:459–464.

Urushidani, T., and J.G. Forte. 1997. Signal transduction and activation of acid secretion in the parietal cell. *J. Membr. Biol.* 159:99–111.

Valentijn, J.A., D. Sengupta, F.D. Gumkowski, L.H. Tang, E.M. Konieczko, and J.D. Jamieson. 1996. Rab3D localizes to secretory granules in rat pancreatic acinar cells. *Eur. J. Cell Biol.* 70:33–41.

Voets, T., E. Neher, and T. Moser. 1999. Mechanisms underlying phasic and sustained secretion in chromaffin cells from mouse

adrenal slices. *Neuron*. 23:607–615.

Wightman, R.M., T.J. Schroeder, J.M. Finnegan, E.L. Ciolkowski, and K. Pihel. 1995. Time course of release of catecholamines from individual vesicles during exocytosis at adrenal medullary cells. *Biophys. J.* 68:383–390.

Zhou, Z., and S. Misler. 1995. Amperometric detection of stimulus-induced quantal release of catecholamines from cultured superior cervical ganglion neurons. *Proc. Natl. Acad. Sci. USA*. 92: 6938–6942.

Zhou, Z., and S. Misler. 1996. Amperometric detection of quantal secretion from patch-clamped rat pancreatic β-cells. *J. Biol. Chem.* 271:270–277.

Zhou, Z., S. Misler, and R.H. Chow. 1996. Rapid fluctuations in transmitter release from single vesicles in bovine adrenal chromaffin cells. *Biophys. J.* 70:1543–1552.